Fe_3O_4 PARTICLES FUNCTIONALIZED WITH EDTA AND PVA - PREPARATION, CHARACTERIZATION AND THEIR USE IN REMOVAL OF MANGANESE IONS FROM SYNTHETIC AQUEOUS SOLUTIONS

Oanamari Daniela ORBULEȚ[1], Claudia BORDA[2*], Delia GARLEANU[3], Gabriel GARLEANU[4], Alexandra STANCU[5], Cristina MODROGAN[6]

In this study, two new types of magnetic materials (Fe_3O_4/EDTA and Fe_3O_4/PVA) were synthesized. Magnetite (Fe_3O_4) particles were synthesized by the simple chemical co-precipitation method. After preparation, the magnetite was functionalized with EDTA (Ethylenediaminetetraacetic acid tetrasodium salt dihydrate) and PVA (Polyvinyl alcohol) through a reaction mechanism with complex formation. The resulting sorbents were characterized using FTIR, TGA/DSG and light microscopy.

FT-IR spectra revealed that the functionalization of EDTA and PVA on the Fe_3O_4 surface was successfully performed fact proved by the presence of -COOH peaks. The use of these sorbents to remove manganese from groundwater has been successful, with a removal efficiency of 99%. High efficiency was obtained at a pH - 6 at room temperature.

Keywords: manganese, Fe_3O_4/EDTA, Fe_3O_4/PVA, groundwater.

1. Introduction

High amounts of manganese can be found mainly in clay soils. The factors that influence the amount of manganese in groundwater are: water flow rate, soil geology, area hydrology, rock composition, quantity and type of bacteria in the soil, etc. [1].

The removal of metal ions from water is a major concern, which has required the development of physical, chemical, physicochemical and biological methods for their selective removal from water. The most effective methods for removing metal ions from aqueous solutions are coagulation-flocculation [2-4],

[1] Lecturer, Faculty of Applied Chemistry and Materials Science, Department of Analytical Chemistry and Environmental Engineering, University POLITEHNICA of Bucharest Bucharest, Romania
[2] Associate professor, Faculty of Industrial Engineering and Robotics, University POLITEHNICA of Bucharest, Romania, e-mail: claudia.borda@upb.ro
[3] Associate professor, Faculty of Industrial Engineering and Robotics, University POLITEHNICA of Bucharest, Romania
[4] Associate professor, Faculty of Industrial Engineering and Robotics, University POLITEHNICA of Bucharest, Romania
[5] Student, University of Medicine and pharmacy "Carol Davila", Bucharest, Romania
[6] Associate professor, Faculty of Applied Chemistry and Materials Science, Department of Analytical Chemistry and Environmental Engineering, University POLITEHNICA of Bucharest, Romania

precipitation [5, 6], flotation [7], ion exchange [8-12], liquid membrane [13], adsorption [14-17], electrochemical methods [18] and biological methods [19-21].

Manganese is an essential trace element necessary for the human body in oxygen metabolism. The maximum allowed dose is 10 mg/day Mn [22]. Exceeding the daily dose leads to local side effects (vomiting, digestive bleeding) or systemic side effects (digestive, respiratory disorders, etc.). In drinking water, the concentration of manganese should not exceed 0.1 mg/L [23].

In general, adsorption can be defined as the accumulation of a substance on the surface or interface between solid adsorbent and contaminant [24]. Gupta et al [25] argue that adsorption and ion exchange involve the transfer of one or more substances between the liquid and solid phase. Physical adsorption occurs when the forces of attraction are weak (van der Waals forces) resulting in a reversible adsorption. Chemisorption occurs when chemical bonds form between the surface of the adsorbent and the adsorbed molecules.

Other forces that control the adsorption processes are hydrophobicity, hydrogen bonds and π - π type interactions.

For an economic process, account must be taken of the nature of the adsorbents, the waste management after use and its operational ease. Magnetic materials have long been of particular scientific and technological interest with a huge potential for application to depollution of the environment, apart from their application in biomedical, biology, electronics, optoelectronics, cosmetics, etc. [26]. The unique characteristics of magnetite (Fe_3O_4) particles and their surface modified with EDTA and PVA are associated with a very high surface-to-volume ratio., low toxicity, biodegradable, biocompatible, ease to synthesize and ease to isolate from solution by applying an external magnetic field [27-30]. The main advantage of using super-paramagnetic iron oxide particles in water purification is that they can be easily removed from the system by applying an external magnetic field.

Recent developments in nanoscience and nanotechnology [31] have shown remarkable potential to address environmental problems. The structured nano-sorbents [32] are far superior to conventional sorbents in terms of efficiency and fast separation speed of wastewater pollutants due to their new properties according to their size. In general, most dissolved pollutants are not magnetic and thus do not respond to the externally applied magnetic field. Nano magnetic particles [33] with large surface area and modified surfaces with special functional ligants with affinity for target pollutants have a potential application in the extraction of pollutants from water [34].

The advancement of the technology regarding the inorganic/organo-metallic syntheses allowed the obtaining of some functionalized nanoparticles/nanomaterials with a controlled particle size. At present, nanomaterials occupy a leading place in the development of nanomaterials, due to

the interesting way of manifesting magnetic, electrical characteristics and potential applications.

The magnetic behaviour of materials is divided into two broad categories depending on how they interact under the action of an external magnetic field (diamagnetic and paramagnetic) [35]. Diamagnetism is characterized by negative magnetic susceptibility, which makes the magnetic moment induced by the action of an external magnetic field less than that of a vacuum. The magnetic moment induced in materials has small values and opposite direction in relation to the applied magnetic field.

As for paramagnetic materials, they consist of atoms that have semi-occupied orbitals with electrons, thus presenting a magnetic dipole. However, the magnetic dipoles are initially randomly oriented in the absence of a magnetic field but, in its presence, they reorient. Paramagnetic materials have a magnetic susceptibility with positive values. Nanometric ferrites have a high adsorption capacity due to the surface and the number of active centers. The affinity of ferrites for an adsorbed compound can be modified by surface functionalization or by total or partial substitution with another metal cation, respectively [36].

2. Materials and methods

All chemical reagents ($FeSO_4 \cdot 7H_2O$, $FeCl_3 \cdot 6H_2O$, NH_3, EDTA, PVA, $MnSO_4$, HNO_3) used in the synthesis and experiments have a high degree of purity and were purchased from Merk and Aldrich Chemical Reagent Co. Ltd. The aqueous solutions were prepared with deionized distilled water. The used glassware was previously washed with 10% volume HNO_3 and then washed thoroughly with deionized distilled water.

2.1. Synthesis of Fe_3O_4/EDTA and Fe_3O_4/PVA

Synthesis of Fe_3O_4/PVA

The precipitation reaction of Fe^{2+} and Fe^{3+} salts ($FeSO_4$ 0.1 M, respectively $FeCl_3$ 0.1 M) with concentrated ammonia (NH_3 25%) without heat treatment leads to the direct obtaining of magnetite, a mixed oxide with an inverted spinel structure. The necessary volumes (in stoichiometric quantities 100 mL) of the two solutions ($FeSO_4$ and $FeCl_3$) calculated to obtain $2.5 \cdot 10^{-3}$ g of Fe_3O_4 are introduced in a Berzelius beaker. Over the obtained solution was added 15 mL of concentrated ammonia, under continuous stirring (200 rpm) (using RSLAB 13 PRO20 Digital Mechanical Stirrer). After that, the reaction mixture was stirred at 200 rpm for another 15 min until the apparition of a black precipitate. The solution on top of the precipitate is immobilized with a magnet placed under the beaker and is decanted. The acquired precipitate was washed three times with 25 mL refined water until the complete removal of chloride ions.

From that point onward, 50 mL 4% PVA solution was added over the mixture and magnetically stirred at 200 rpm for 20 min at room temperature. After the blending time has passed, the solution was filtered and rinsed with distilled water and afterwards was transferred, in order to dry, to a watch bottle (weighed beforehand). The precipitate was slowly heated in the oven (Multi-lab ML-LE 15/11) at 100 °C. After gelling, the temperature was increased at 150 °C and heating continued in the oven for 4 h. The resulting sample (Fe_3O_4/PVA) was very well crushed before being used for the adsorption tests and characterized [35].

Synthesis of Fe_3O_4/EDTA

After preparation of the magnetite 0.615 mg of ethylene-diamine-tetra-acetic acid (EDTA) (Merk) is added as a precipitating agent and as a coating agent under continuous stirring at 200 rpm. From the literature data, a mass ratio of 1:1 Fe_3O_4:EDTA was chosen to ensure that the Fe_3O_4 surface was completely covered. To complete the reaction, stirring is continued for 1 h at 50 °C (in the FC-302 incubator). Finally, the formed product was washed with deionized distilled water and dried at 80 °C for 3 h [36].

2.2. Characterization of the synthesized materials

Optical microscopy analysis was used on both Fe_3O_4/EDTA and Fe_3O_4/PVA to observe the structural properties of the Fe_3O_4/EDTA and Fe_3O_4/PVA regarding the adsorption of Mn^{2+}. The analysis of the phase composition of the sorbents was performed by Media-Tech MT4096, USB, magnification 400x.

The Thermal Gravimetric Analysis (TGA) and Differential Scanning Calorimetric measurement (DSC) of the Fe_3O_4/PVA was conducted using a Q5000IR (TA Instruments). The samples of powder (7–15 mg) were heated from 40 to 700 ° C under nitrogen atmosphere (50 mL/min) with a heating rate of 10°C/min in platinum pans (100 µL). For highlighting the formation of magnetite in the synthesized samples FT-IR spectroscopy was the used technology. FTIR spectra were recorded using the Jasco FTIR 6300 spectrometer equipped with a Golden Gate Specac ATR (KRS5 lens), in the range of 400-4000 cm^{-1} (32 scans at 4 cm^{-1} resolution). The DE-convolution of the spectra was performed using the Jasco spectrum analysis program.

Table 1.

Notation of samples before and after adsorption of Mn^{2+}

Samples	Notation
Fe_3O_4/EDTA blank	P1
Fe_3O_4/PVA blank	P2
Fe_3O_4/EDTA – Mn^{2+}	P3
Fe_3O_4/PVA – Mn^{2+}	P4

2.3. Adsorption study of Mn^{2+} onto Fe_3O_4/EDTA and Fe_3O_4/PVA

For the kinetic studies, the experimental procedure started by placing 0.5 g Fe_3O_4/EDTA; Fe_3O_4/PVA in Berzelius glasses and then adding 50 cm^3 $MnSO_4$ solution with concentration of 80 and 40 mg/L. The glasses were coated in order to stop the evaporation and were stirred (200 rpm) at several times (5, 10, 20, 30, 60, 90 min) at 20 °C. Stock solutions containing Mn^{2+} were prepared by dissolving $MnSO_4$ in deionized water at room temperature (20 ± 2 °C). By diluting the stock solutions with deionized water and H_2SO_4 or NaOH in order to adjust the pH to the preset values, we obtained the working solutions.

Afterwards, 10 cm^3 solution from the filtrate was spectrophotometrically analyzed at λ = 525 nm (Shimatzu 1900 UV-VIS). Fe_3O_4/EDTA; Fe_3O_4/PVA was used like powder and boring.

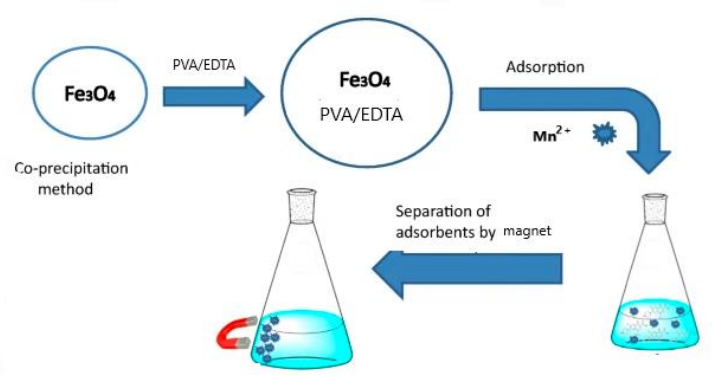

Fig. 1. Adsorption study of manganese ions used Fe_3O_4/EDTA and Fe_3O_4/PVA

Mechanic blending was realised by means of a Heidolph Unimax shaker at 200 rpm. When the mixing procedure was over, the samples were sifted using blue ribbon paper and the obtained solution was placed in 50 mL volumetric flask. From the extract, 10 cm^3 solution was spectrophotometrically analyzed at λ = 525 nm. All the experiments were performed at pH = 7 (pH-meter JKI JK-PH009, 0 - 14 pH).

Kinetic study of Mn^{2+}- Fe_3O_4/EDTA or Fe_3O_4/PVA

The models used to calculate the time load are:

- A **pseudo-order II kinetic adsorption model** (Demirbas, 2004):

$$\frac{dq_t}{dt} = k_2(q_e - q_t)^2 \quad (1)$$

where: k_2 = pseudo-order type II rate constant of the process(g/min·mg); q_e = loading of the iron particles with manganese at equilibrium, (mg/g); q_t = loading of the iron particles with manganese (adsorption capacity) at time t, (mg/g).

Putting the condition of the limit: t = 0, t = t şi $q_t = 0$, $q_t = q_t$ by integrating equation (1) we obtained:

$$\int_0^{q_t} \frac{dq_t}{(q_e - q_t)^2} = k_2 \int_0^t dt \Rightarrow \frac{1}{q_e - q_t} - \frac{1}{q_e} = k_2 \cdot t \quad (2)$$

- A **pseudo-order type I kinetic adsorption model**, (Demirbas, 2004):

$$\frac{dq_t}{dt} = k_1(q_e - q_t) \quad (3)$$

Putting the condition of the limit: t = 0, t = t şi $q_t = 0$, $q_t = q_t$ by integrating equation (3) we obtained:

$\log(q_e - q_t) = \log(q_e) - \frac{k_1}{2{,}303} t$, where k_1 şi q_e can be determined from the slope and intercept of the line.

The model used to determine the *evolution of load over time* is given by the balance equation (4)

$$q = \frac{V_{aq} \cdot (C_0 - C)}{m_n} \quad (4)$$

where: q_t *şi* C – have the same significance as in equation (2), (mg/g); C_0 = the initial concentration of Mn^{2+} in aqueous phase, mg/L; V_{aq} = the volume of the aqueous phase, mL; m_n = the mass of the functionalized iron particles, g.

The proposed models, especially their parameters, can be input data for the elaboration of mathematical models that would describe more fully the behavior of manganese ions in water. This phenomenon was described based on the calculated parameters, as well as by using pseudo order I and II kinetic models, which were tested with experimental data and whose curves were compared with the experimental curves.

3. Results and discussion

3.1. Characterization of Fe_3O_4/EDTA; Fe_3O_4/PVA

Both the original and modified magnetite (Fe_3O_4/PVA) were analyzed using FTIR-spectroscopy in order to attest the formation of the Fe_3O_4. The FTIR spectra indicated a significative modification of the absorption bands between the samples (Fig. 2).

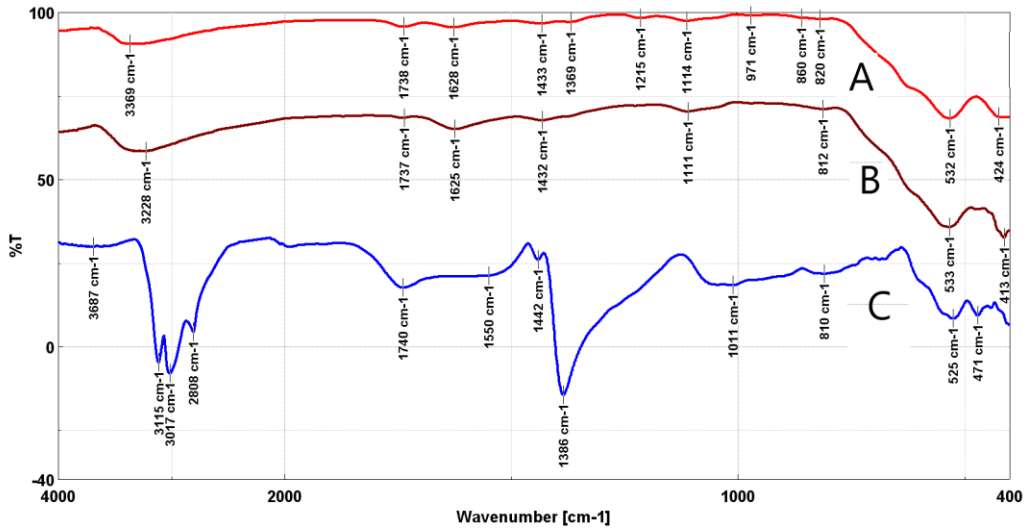

Fig. 2. FT-IR spectra of Fe_3O_4 (A), Fe_3O_4/EDTA (B) and Fe_3O_4/PVA (C)

Fourier transformed infrared spectrometry (FTIR) and thermogravimetry (TGA) were used to characterize all of the obtained materials. In this respect, the FTIR spectra (sample B) show peaks for N-H (3228 – 3369 cm^{-1}), C=O (1625 – 1628 cm^{-1}), C-N (1432 – 1433 cm^{-1}), and C-NH_2 (1111 – 1114 cm^{-1}), and Fe-O (413 – 533 cm^{-1}). The new peaks appearing in the EDTA/Fe_2O_3 spectrum, namely C-C (860 cm^{-1}), [N(-CH_2-)$_3$] (971 cm^{-1}), and (C-O) COOH (1369 cm^{-1}) are attributed to the newly activated EDTA molecules on the magnetic particles' surface. PVA was shown to have been successfully embedded and incorporated into Fe_3O_4 particles' surface by the FT-IR spectra. The FT-IR spectrum indicates the presence of two peaks at 532 cm^{-1} (sample A) and 525 cm^{-1}, respectively, (sample C) that confirm the formation of the Fe_3O_4 spinel oxide. They are caused by the stretching vibrations of the Fe-O bonds. The weak shoulder at 421 cm^{-1} (sample A) and 471 cm^{-1} (sample C) can be easily observed and is attributed to the magnetite [1]. The absorption band at 815 cm^{-1} (sample A) and 810 cm^{-1} (sample C), respectively, corresponds with bending vibration related to the out of the plane bonds of O-H. The bands at ~1740 cm^{-1} and 1628 cm^{-1} are assignable to the stretching vibration of C=O from the COOH group. The absorption band at 1436 cm^{-1} (sample A) and 1442 cm^{-1} (sample C) refers to asymmetric C-H stretching [38].

The vibration mode of C-O noticeable in the spectrum at 1370 cm^{-1} is assigned to HCO_3^-, which indicates that the sample contained carbonate contaminants [37]. Successful coating of Fe_3O_4 by PVA was designated by the presence of hydroxyl (O–H) (stretching from the intermolecular and intramolecular hydrogen bonds), carbonyl (C–C), and Fe–O–C bonds vibrations (sample B), in the region of ~3700 cm^{-1}, ~2300 cm^{-1}, and 1550 cm^{-1}. Also, the

interaction of the surface of Fe_3O_4 with PVA could be identified by the presence of Fe–O–C stretching in the region of 1120-1090 cm^{-1} [38]. The FTIR of sample B revealed peaks at 3017 cm^{-1} and 2808 cm^{-1}, respectively, that refer to the C-H stretching of the alkyl groups. The absorption bands observed at 1740 cm^{-1} and 1386 cm^{-1} were related to carbonyl and methylene stretching, respectively. These results were in agreement with other reported in literature [39].

TGA-DSC thermal analysis (sample A) was the first technology to characterize the powders obtained (Fe_3O_4/PVA) by drying precipitates in an oven for 24 h. Based on the exothermic process of oxidation of Fe (II) to Fe (III), with an increase of the mass, which occurs up to 200 °C [37], thermal analysis can highlight the presence of magnetite in the newly formed powders. Because of the low temperature the process required, the obtained powders may have an important amount of -OH groups on their surface; this explains why the endothermic process of removing the -OH groups from the surface and H_2O molecules can overlap with the oxidation process. Therefore, it is indeed difficult to potentially quantify the content in magnetite in the analyzed powder. Despite all of this, the presence of this exothermic process with increasing mass can be considered as a fingerprint for the presence of magnetite.

Three weight loss steps were shown on the thermogram of EDTA/Fe_3O_4 (sample B), which could also be connected to the presence of EDTA. The first two weight losses, 3.07% (Fe_3O_4) and 4.31% (EDTA/Fe_3O_4), at temperature bellow 200 °C are attributed to the dehydration process. The weight loss between 200 and 500 °C, as it is visible on EDTA/Fe_3O_4 thermogram, is attributed to the complete decomposition of EDTA mostly due to pyrolysis and oxidation. All these findings suggest that the EDTA was successfully pinned on the surface of magnetite particles.

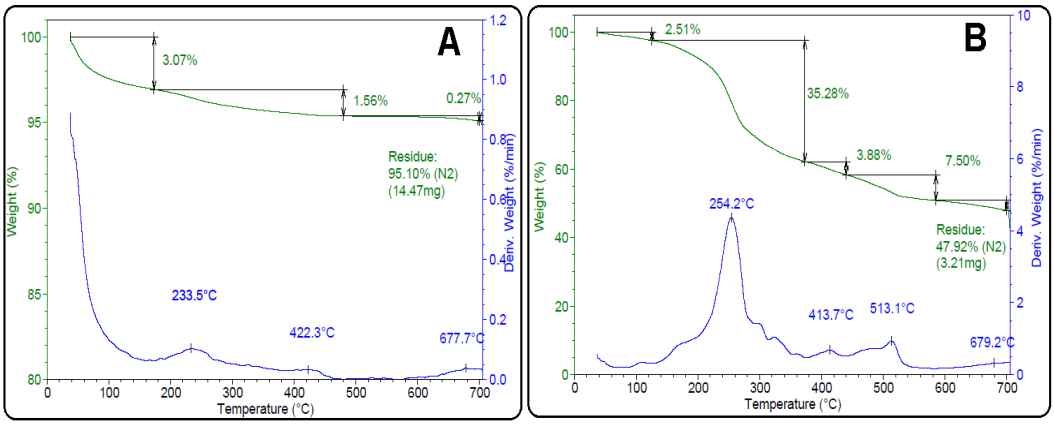

Fig. 3. TGA-DSC curves of the obtained powders: Fe_3O_4/PVA (A) and Fe_3O_4/EDTA (B)

In all initial samples, the presence of magnetite is highlighted by the TGA-DSC curves. The existence of magnetite was confirmed by the exothermic process with mass increase in the temperature range 100-190 °C, corresponding to the oxidation of Fe_3O_4 at γ-Fe_2O_3 (on paper, for pure magnetite, the increase in its mass should be 3.45%). An endothermic process with mass loss precedes this process, because of the elimination of water molecules bound to the surface of the particles by hydrogen bonds. This process coincides with the oxidation of magnetite. A small mass increase (+ 0.14%) in the range of 100-180 °C (the highest exothermic effect being located at 120 °C) is shown by the samples that were obtained using NH_3 as a precipitant. This may be due to the overlapping of another weak exothermic process at ~170 °C that occurs with mass loss and is possibly connected to the removal of NH_3 that remained bounded on the particles' surface.

Although there are no significant thermal effects, the loss of mass up to 400 °C may be due to the DE-hydroxylation process. Another exothermic process, without mass exchange, occurs around 560 °C and corresponds to the transition of maghemite (γ- Fe_2O_3) to hematite (α- Fe_2O_3).

The investigation of the surface morphology of the prepared Fe_3O_4/EDTA and modified magnetite (Fe_3O_4/PVA) was performed by means an optical digital microscope (Media-Tech MT4096, USB).

The surface morphology of the original (Fe_3O_4) and modified magnetite (Fe_3O_4/PVA), was examined using an optical digital microscope (Media-Tech MT4096, USB, magnification 400x) (Fig. 4).

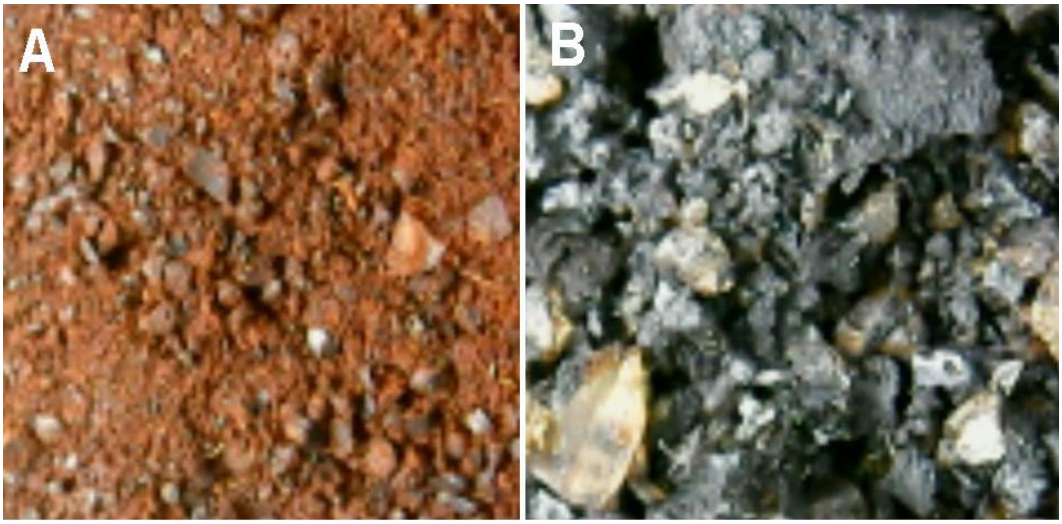

Fig. 4. Surface morphology images of the samples: Fe_3O_4/EDTA (A) and Fe_3O_4/PVA (B).

The images of the surfaces show the existence of Fe_3O_4/EDTA agglomerations, where the magnetic particles can be more or less united together and are almost spherical shaped, but although not very regular. Also, the images depict that the particles don't have an even distribution presenting different shapes and sizes. The surface image of the Fe_3O_4/PVA indicated very clearly how the particles are formed and dispersed, process which was consistent with the reported coated magnetic particles. Also, it is noticed that the Fe_3O_4 particles have been stabilized by adding PVA on their surface to prevent them from coagulating. The affinity of the particles to the cross linker had also been enhanced [40].

a. Effect of pH

The pH is an important factor that affects the adsorption process by tangling with the structure of the pollutant and the surface charge of the adsorbent [37]. This influence of pH is related to the form of the metal ion in the solution, as well as to the functional grouping of the extractant.

In Fig. 5 it is presented the effect that the pH has on the removal of Mn2+ from waters. As the pH increases, the efficiency of Mn2+ removal decreases., so that the greatest extent of the removal in pH = 6 is more than 90%. The results of this study are similar to those of other researches. Also, the study performed by Khaniabadi (2017) showed that increasing the pH decreases efficiency [39].

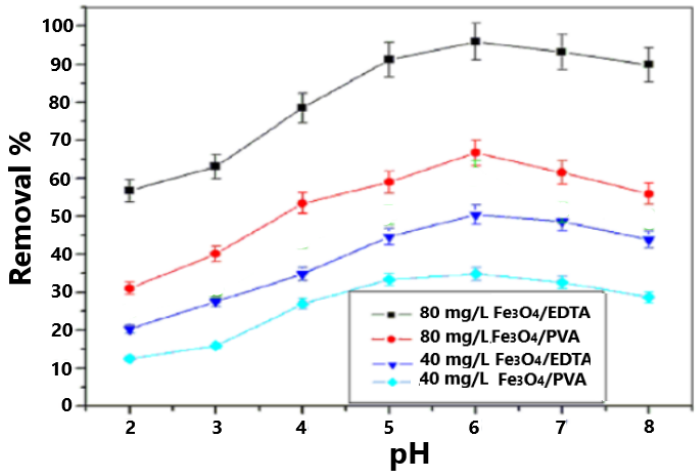

Fig. 5. The effect of pH on the performance of Mn^{2+} removal using Fe_3O_4/EDTA and Fe_3O_4/PVA (V = 50 mL. adsorbent mass 0.5 g, C_0 = 80 and 40 mg/L, t = 60 min)

b. Kinetics adsorption evaluation

A more accurate quantification of the influences of adsorption processes has been achieved by laboratory evaluation tests on static models.

Among the models proposed for testing, it was found that the pseudo order II kinetic model is the most suitable for describing the adsorbtion process, for this model

obtaining a determination coefficient, $R^2 \sim 1$. The removal rate of manganese ions was about 99% in a short time, about 5 min. The kinetic parameters calculated by bilinear regression according to the mathematical models used are presented in table 2. The kinetic curves obtained experimentally for Mn^{2+} sorption on Fe_3O_4/EDTA and Fe_3O_4/PVA are presented in Fig. 6. From the analysis of the curves presented in Fig. 6 it is observed that: the most significant decrease of the concentration occurs in the first 5-10 min. After 10 min, the concentration of manganese ions in the solution decreases by 0.1%, then the decrease is slow, becoming constant after 1 h.

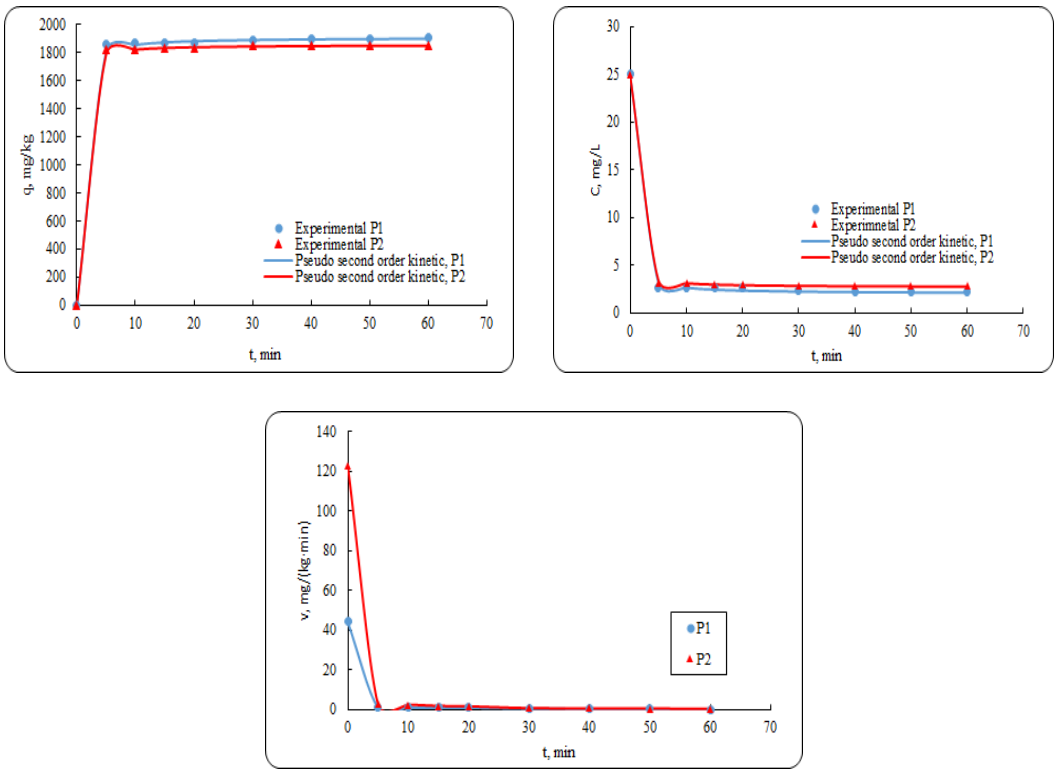

Fig. 6. Integral kinetic curves for Mn^{2+} retention on Fe_3O_4/EDTA (1-3) and Fe_3O_4/PVA at 20 °C

The rate of reduction of manganese ions was very fast in the initial period, in the first 5 min, then the reactivity was lower after a certain time, due to the decrease of the available free exchange positions. From the point of view of the charge of the two adsorbents Fe_3O_4/EDTA and Fe_3O_4/PVA they showed a similar behavior, with the observation that the adsorbent Fe_3O_4/EDTA offered several free positions so that the manganese ions achieved a higher charge of the surface of 1905 mg/kg, compared to the Fe_3O_4/PVA adsorbent which led to a maximum load of 1883.33 mg/kg.

Pseudo-first-order and pseudo-second-order models described by Equations 5, 6, 7 [17] were used to evaluate the kinetic sorption data. The kinetic parameters and the determination coefficients are presented in table 2 and Fig.s 7-8.

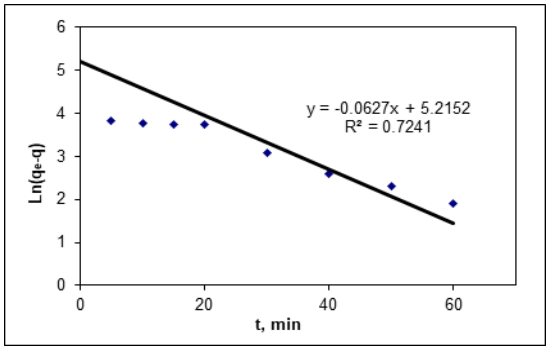

Fig. 7. Interpolation line for determining the parameters of the pseudo order I kinetic model for sample P1.

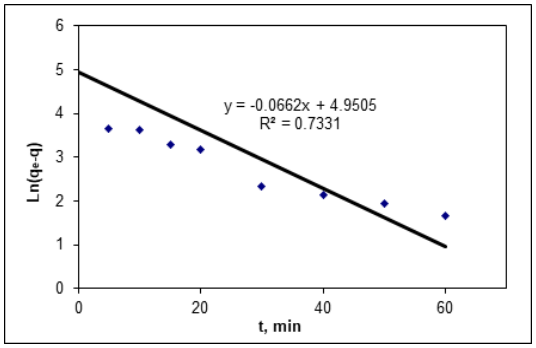

Fig. 8. Interpolation line for determining the parameters of the pseudo order I kinetic model for sample P2.

According to the determination coefficients (R^2) the kinetic sorption of Mn^{2+} was better evaluated by the pseudo-second-order kinetic model for all experiments. The kinetic rate (k_2) is always higher for 0.662 (table 2).

Table 2.

Kinetic parameters and the determination coefficients of Mn^{2+} sorption on Fe_3O_4/EDTA (samples P1) and Fe_3O_4/PVA (sample P2), at 20°C

Kinetic model	Parameters	Sample P1 20°C	Sample P2 20°C
Experimental	$q_{e,exp.}$	1905	1883.33
Pseudo-first order	$q_{e,calc.}$ k_1, min^{-1} R^2	1911.719 0.0627 0.7241	1858.59 0.0662 0.7331
Pseudo-second order	$q_{e,calc.}$ k_2, min^{-1} R^2	1911.719 0.001867 1	1858.59 0.002876 1

A higher sorption rate was observed at the initial reaction time when 80 mg/L of Mn^{2+} was employed. At 60 min of shaking time, 15%, and 95% of Mn^{2+} were removed for the initial concentration. The presence of PVA reduces the number of free active centers on the surface of the functionalized Fe_3O_4 material, thus preventing manganese ions from being adsorbed, which reduces the adsorption capacity to 1883.33 mg/kg. These results indicate a higher affinity between Mn^{2+} and the available active sorption sites of Fe_3O_4/EDTA, leading to

faster sorption compared to Fe_3O_4/PVA. In addition, the absorption capacity of the functionalized Fe_3O_4 material follows the same increased adsorption trend in the case of sample P1 and sample P2 suggesting that the existence of functional groups with oxygen on its surface have an important role in increasing the absorption capacity (table 2).

The experiments were modeled using different kinetic models, pseudo-order I and pseudo-order II models. According to the correlation coefficients (R^2), the kinetic sorption of Mn^{2+} was better evaluated by the pseudo-order II kinetic model for all experiments. The obtained results indicated that the Mn^{2+} adsorption was governed by a pseudo-order II kinetic model. These are confirmed by correlation coefficients that were equal to 1. This kinetic model indicates that chemical adsorption or chemical bonding between the adsorbent active sites and manganese ions could dominate the adsorption process. The result demonstrated that the prepared Fe_3O_4/EDTA exhibited an excellent adsorbent capacity for Mn^{2+} (1905 mg/kg, initial Mn^{2+} concentration of 80 mg/L) than other adsorbents such as kaolinite (0.446 mg/g) [42], riccia xuitans (0.254 mg/g) [43], bombax malabaricum (0.2837 mg/g), ipomea batatas (0.3627 mg/g), pithecelobium dulse (0.4156 mg/g), peltaforum ferraginium (0.4433 mg/g) [44].

4. Conclusions

The purpose of this work was to synthetize, characterize and apply an Fe_3O_4/EDTA/ Fe_3O_4/PVA for removing Mn^{2+} from synthetical wastewaters, similar to groundwaters. The pH effect, initial concentration of Mn^{2+} and the adsorption kinetics were also examined. The success of the synthesis of the new material has been confirmed by FTIR, optical microscopy and TGA/DSG analysis that revealed new properties comparative with the basic material, namely magnetite.

When it comes to the adsorption of Mn^{2+}, the equilibrium can be reached quickly, in about 60 min of shaking time. The pseudo-second-order expression accurately described the Mn^{2+} adsorption kinetics for the prepared Fe_3O_4/EDTA and Fe_3O_4/PVA. The adsorption capacity of Mn^{2+} increased with increasing the initial Mn^{2+} concentration. The adsorption experiments also revealed that Fe_3O_4/EDTA has a higher adsorption capacity than Fe_3O_4/PVA for Mn^{2+}. Moreover, the high rate of adsorption of the three chemical species has been highlighted. In this regard, about 95% of them was removed from the aqueous solution in about 60 min.

The obtained results prove that the synthetized Fe_3O_4/EDTA can be used as potential adsorbent for the removal of Mn^{2+} from wastewater.

Acknowledgments

This work has been funded by University Politehnica of Bucharest, through the "Excellence Research Grants" Program, UPB – GEX 2017. Identifier: UPB- GEX2017, Ctr. No. 78/2017 Cod 136".

R E F E R E N C E S

[1]. *J.E. Tobiason, A. Bazilio, J. Goodwill, X. Mai, C. Nguyen,* Manganese Removal from Drinking Water Sources, Water Pollution, 2, pp. 168–177, 2016.

[2]. *Z. Fu-wang, Li Xing, Y. Yan-ling,* Study on the effect of manganese (II) removal with oxidation and coagulation aid of potassium manganate, Bioinformatics and Biomedical Eng ICBBE, 3rd International Conference, pp. 1-4, 2009.

[3]. *X. Tang, H. Zheng, H. Teng, Y. Sun, J. Guo, W. Xiea, Q. Yang, W. Chen,* Chemical coagulation process for the removal of heavy metals from water: a review Desalin. Water Treat. , pp. 1-16, 2014.

[4] *D.S. Patil, S.M. Chavan, J.U. Kennedy, Oubagaranadin,* A review of technologies for manganese removal from wastewaters, Journal of Environmental Chemical Engineering, Volume 4, Issue 1, pp. 468-487, 2016.

[5] *L. Pietrelli, N. MariaIppolito, S. Ferro, V.G. Dovì,,* Removal of Mn and As from drinking water by red mud and pyrolusite, Journal of Environmental Management, Volume 237, pp. 526-533, 2019.

[6] *A.M. Silva, E.C. Cunha, F.D.R. Silva, V.A. Leão,* Treatment of high-manganese mine water with limestone and sodium carbonate, J. Cleaner Prod. 29-30, pp. 11–19, 2019.

[7]. *H. Polata, D. Erdogan,* Heavy metal removal from waste waters by ion flotation, J. Hazard. Mater. 148 , pp. 267–273, 2007.

[8]. *O.N. Kononova, G.L. Bryuzgina, O.V. Apchitaeva, Y.S. Kononov*, Ion exchange recovery of chromium (VI) and manganese (II) from aqueous solutions, Arab. J. Chem., 2015.

[9]. *W. Zhang, C.Y. Cheng, Y. Pranolo,* Investigation of methods for removal and recovery of manganese in hydrometallurgical processes. Hydrometallurgy, *101,* 58-63, 2010.

[10]. *H.A. Aziz, P.G. Smith,* Removal of manganese from water using crushed dolomite filtration technique. Water Res., *30,* 489-492, 1996.

[11]. *A.M. Silva, E.C. Cunha, F.D.R. Silva, V.A. Leão,* Treatment of high-manganese mine water with limestone and sodium carbonate., J. Clean. Prod., 29–30, 11-19, 2012.

[12]. *H. Yang, Z. Yan, X. Du, L. Bai, H. Yu, A. Ding, G. Li, H. Liang, T.M. Aminabhavi,* Removal of manganese from groundwater in the ripened sand filtration: Biological oxidation versus chemical auto-catalytic oxidation, Chemical Engineering Journal Volume 382, 2020.

[13]. *L. Caixeta, F. Layse, C. Ferreira, V.L. Cardoso, U. Coutinho Filho,* Mn(II) removal from water using emulsion liquid membrane composed of chelating agents and biosurfactant produced *in loco*, Journal of Water Process Engineering, Volume 29, 100792, 2019.

[14]. *B. Kwakye-Awuah, B. Sefa-Ntiri, E. Von-Kiti, I. Nkrumah, C. Williams,* Adsorptive removal of iron and manganese from groundwater samples in Ghana by zeolite y synthesized from bauxite and kaolin. Water (Switzerland) 11, 2019.

[15]. *V.K. Gupta, P.J.M. Carrott, M.M.L. Ribeiro Carrott,* Suhas Low-Cost Adsorbents: Growing Approach to Wastewater Treatment. Critical Reviews in Environmental Science and Technology, 39, pp. 783-842., 2009.

[16]. *M.Á. Lobo-Recio, C. Rodrigues, T.C. Jeremias, F.R. Lapolli, I. Padilla, A. López-Delgado,* Highly efficient removal of aluminum, iron, and manganese ions using Linde type-A zeolite obtained from hazardous waste, Chemosphere, 267, pp. 128919, 2021.

[17]. *I.L. Calugaru, T. Genty, C.M. Neculita*, Treatment of manganese, in the presence or absence of iron, in acid and neutral mine drainage using raw vs half-calcined dolomite, Minerals Engineering, 160, pp. 106666, 2021.

[18]. *M. Ince*, Treatment of manganese-phosphate coating wastewater by electrocoagulation, Sep. Sci. Technol., 48, pp. 515-522, 2013.

[19]. *M. Han, Z. Zhao, W. Gao, F. Cui*, Study on the factors affecting simultaneous removal of ammonia and manganese by pilot-scale biological aerated filter (BAF) for drinking water pre-treatment., Bioresour. Technol., *145*, pp. 17-24., 2013.

[20]. *M.A. Robinson-Lora, R.A. Brennan*, Anaerobic precipitation of manganese and coexisting metals in mine impacted water treated with crab shell-associated minerals., Appl. Geochem. 26, pp. 853–862, 2011.

[21]. *Y. Li, Z. Xu, H. Ma, A.S. Hursthouse*, Removal of Manganese(II) from Acid Mine Wastewater: A Review of the Challenges and Opportunities with Special Emphasis on Mn-Oxidizing Bacteria and Microalgae Water, 11, pp. 2493 2019.

[22]. *C. Modrogan, S. Căprărescu, A.M. Dăncilă, O.D. Orbuleț, E. Vasile, V. Purcar*, Mixed Oxide Layered Double Hydroxide Materials: Synthesis, Characterization and Efficient Application for Mn^{2+} Removal from Synthetic Wastewater, Materials, *13* (18), pp. 4089; 2020.

[23]. *O.F. Dávila, J.T. Torres, A.F. Valdes*, Effect of Mg Concentration on the Aluminothermic Reduction of Mn_2O_3 Particles Obtained from Cathodes of Discharged Alkaline Batteries: Mathematical Modeling and Experimental Results, Metals, *9*, pp.49-64, 2019.

[24]. *R. Sanghi,; P. Verma*, Decolorisation of aqueous dye solutions by low-cost adsorbents: a review. *Coloration Technology*, 129, pp. 85-108, 2013.

[25]. *H. Gupta, P.R. Gogate*, Intensified removal of copper from waste water using activated watermelon based biosorbent in the presence of ultrasound, Ultrason Sonochem, 30, pp. 113-22, 2016.

[26]. *P.N. Oliveira, R.D. Bini, G.S. Dias, P. Alcouffe, I.A. Santos, L. David, L.F. Cótica*, Magnetite nanoparticles with controlled sizes via thermal degradation of optimized PVA/Fe(III) complexes, Journal of Magnetism and Magnetic Materials 460 ,pp. 381–390, 2018.

[27]. *F. Sadeghfarb, M. Ghaedi, A. Asfaram, R. Jannesar, H. Javadian, V. Pezeshkpour*, Polyvinyl alcohol/Fe_3O_4@carbon nanotubes nanocomposite: Electrochemical-assisted synthesis, physicochemical characterization, optical properties, cytotoxicity effects and ultrasound-assisted treatment of aqueous based organic compound, Journal of Industrial and Engineering Chemistry 65, pp. 349–362, 2018.

[28]. *M. Stoia, R. Istratie,* C. *Păcurariu*, Investigation of magnetite nanoparticles stability in air by thermal analysis and FTIR spectroscopy. J Therm Anal Calorim 125, pp. 1185–1198, 2016.

[29]. *S. Nigam,; K.C. Barick, D. Bahadur,* Development of citrate stabilized Fe_3O_4 nanoparticles: Conjugation and release of doxorubicin for the therapeutic applications. J. Magn. Magn. Mater., 323, pp. 237-243., 2011

[30]. *K. Tharani, L.C. Nehru*, Synthesis and characterization of iron oxide nanoparticle by precipitation method. Int J Rec Adv Phys Sci, 2, pp. 47-50, 2015.

[31]. *A. Sabarudin, R. Wahid, F.C. Nalle, R.A. Shobirin, D.J.D.H. Santjojo*, Designed structure and magnetic characteristic studies of magnetic iron oxide (Fe_3O_4) nanoparticles coated by polyvinyl alcohol and polyvinyl alcohol-linked with glutaraldehyde, Rasayan J. Chem., 10(4), pp.1261-1270, 2017.

[32]. *M. Olukman, O. Şanli, E.K. Solak*, Synthesis of magnetite in poly(vinyl alcohol) matrix and its use in separation of acetone/water mixtures via pervaporation, vapor permeation with and without temperature difference methods, Vacuum 120, pp.107-115, 2015.

[33]. *Y. Mansoori, A. Khodayari, A. Banaei, M. Mirzaeinejad, Y. Azizian-Kalandaragh, M. Pooresmaeil*, Fe_3O_4–PVAc nanocomposites: surface modification of sonochemically

prepared magnetite nanoparticles via chemical grafting of poly(vinyl acetate), RSC Adv. 6, pp. 48676- 48683, 2016.

[34]. *H. Yan, H. Li, X. Tao, K. Li, H. Yang, A. Li, S. Xiao, R. Cheng,* Rapid Removal and Separation of Iron(II) and Manganese(II) from Micropolluted Water Using Magnetic Graphene Oxide, ACS Appl. Mater. Interfaces, 6, 12, pp.9871–9880, 2014.

[35]. *I. Ali, M. Islam, M. Ashiq, I. Shakir, N. Karamat, M. Ishaque, M.N. Akhtar, H.M. Khan, M. Irfan, M.A. Khan*, Investigation of the magnetic properties of nanometric SrSmCoNi ferrite/PST matrix, Ceramics International 41(7), pp. 8748-8754, 2015.

[36]. *M. Aghazadeh, I. Karimzadeh, M.R. Ganjali*, Ethylenediaminetetraacetic acid capped superparamagnetic iron oxide (Fe_3O_4) nanoparticles: A novel preparation method and characterization, Journal of Magnetism and Magnetic Materials, Volume 439, pp. 312-319, 2017.

[37] *M.A. Ahmed, N. Okasha, S.I. El-Dek*, Preparation and characterization of nanometric Mn ferrite via different methods, Nanotechnology, Volume 19, Number 6, 2008.

[38]. *H. Lin, Y. Watanabe, M. Kimura, K. Hanabusa*, Preparation of magnetic poly(vinyl alcohol) (PVA) materials by in situ synthesis of magnetite in a PVA matrix, Journal of Applied Polymer Science 87(8), pp. 1239 – 1247, 2003.

[39]. *T. Gong; Y. Tang*, Preparation of multifunctional nanocomposites Fe_3O_4@SiO_2–EDTA and its adsorption of heavy metal ions in water solution, Water Sci Technol 81 (1), pp. 170–177, 2020

[40]. *N. Habibi*, Preparation of biocompatible magnetite-carboxymethyl cellulose nanocomposite: Characterization of nanocomposite by FTIR, XRD, FESEM and TEM, Spectrochimica Acta Part A: Molecular and Biomolecular Spectroscopy, Volume 131, pp. 55-58, 2014.

[41]. *M. Muniz-Miranda, F. Muniz-Miranda, E. Giorgetti*, Spectroscopic and Microscopic Analyses of Fe_3O_4/Au Nanoparticles Obtained by Laser Ablation in Water, Nanomaterials , *10*(1), pp. 132, 2020.

[42]. *O. Yavuz, Y. Altunkaynak, F. Guze*, Removal of copper, nickel, cobalt and manganese from aqueous solution by kaolinite. Water. Res., 37(4), pp. 948-952, 2003.

[43]. *K. Chojnacka*, Bioaccumulation of Cr (III) ions by blue-green alga *Spirulina* sp. Part I. A comparison with biosorption. *Am. J. Agric. Biol. Sci.*, 2, pp. 218-223, 2007.

[44]. *K.A. Emmanuel, A.V. Rao*, Comparative Study on Adsorption of Mn(II) from Aqueous Solutions on Various Activated Carbons. E-J. Chem., 6(3), pp. 693–704, 2009.